ROP INTERACTIVE PARTNER b interacts with the ROP GTPase RACB and supports fungal penetration into barley epidermal cells

Christopher McCollum, Stefan Engelhardt, Ralph Hückelhoven[#]

Phytopathology, TUM School of Life Science Weihenstephan, Technical University of Munich, Emil-Ramann Str.2, 85354 Freising, Germany

[#]Corresponding author: hueckelhoven@wzw.tum.de

Abstract

RHO of Plants (ROP) G-proteins are key components of cell polarization processes in plant development. The barley (*Hordeum vulgare*) ROP protein RACB, is a susceptibility factor in the interaction of barley with the barley powdery mildew fungus *Blumeria graminis* f.sp. *hordei* (*Bgh*). RACB also drives polar cell development, and this function might be coopted during formation of fungal haustoria in epidermal cells of barley. In order to understand RACB signaling during the interaction of barley with *Bgh*, we searched for potential downstream interactors of RACB. Here, we show that ROP INTERACTIVE PARTNER b (RIPb) directly interacts with RACB in yeast and *in planta*. Over-expression of RIPb supports susceptibility of barley to *Bgh*. RIPb further interacts with itself at microtubules. However, the interaction with activated RACB takes place at the plasma membrane. Both, RIPb and RACB are recruited to the site of fungal attack around the neck of developing haustoria suggesting locally enhanced ROP activity. We further assigned different functions to different domains of the RIPb protein. The N-terminal coiled-coil CC1 domain is required for microtubule localization, while the C-terminal coiled-coil CC2 domain is sufficient to interact with RACB and to fulfill a function in susceptibility at the plasma membrane. Hence, RIPb appears to locate at microtubules and is then

recruited by activated RACB for a function at the plasma membrane during formation of the haustorial complex.

Introduction

The interaction of plants with powdery mildew fungi is a model for the biology of cell-autonomous responses to fungal parasites (Dörmann et al. 2014). The powdery mildew fungus *Blumeria graminis* f.sp. *hordei* (*Bgh*) is a biotrophic ascomycete specifically adapted to barley (*Hordeum vulgare*) and grows largely on the plant´s surface. In the beginning of its life cycle it has to penetrate a single epidermal cell in order to establish a haustorium for nutrient uptake (Hahn et al. 1997, Voegele et al. 2001) and to provide a surface for the translocation of virulence effector proteins into the host cell (Catanzariti et al. 2007). During all stages of fungal invasion, the host cell stays intact. Host cytosol and fungal haustorium are separated by the extrahaustorial matrix and the extrahaustorial membrane (EHM), which derive from the plant.

Plant host cells polarize in very early phases of the interaction with fungi. A reorganization of the cytoskeleton was shown in different pathosystems, as well as the accumulation of peroxisomes, mitochondria, Golgi bodies and ER at the site of pathogen attack (Kobayashi et al. 1997, Takemoto et al. 2003, Koh et al. 2005, Takemoto et al. 2006, Fuchs et al. 2016). This is accompanied by relocation of the nucleus to the site of attack (Gross et al. 1993, Scheler et al. 2016). Polarization is considered important for effective defense, in particular for the focal formation of papilla or cell wall appositions, which requires localized deposition of callose, other cell wall glucans and phenolic compounds at the attempted penetration site (McLusky et al. 1999, Hückelhoven 2007, Chowdhury et al. 2014). However, it is reasonable to assume, that host cell polarization is also important for successful pathogen establishment, for instance for the generation of the EHM (Scheler et al. 2016, Kwaaitaal et al. 2017).

ROP GTPases (RHO of Plants, also called RAC for rat sarcoma–related C3 botulinum toxin substrate) are small monomeric G-proteins that form a RHO subfamily, which is exclusively present in plants. ROPs can cycle between an actively signaling GTP-bound state and an inactive GDP-bound state and are crucial for polarity of diverse types of plant cells (Feiguelman et al. 2018). ROPs seem to fulfill different functions depending on the interacting downstream factors called ROP-effectors. For instance *Arabidopsis thaliana* ROP2 suppresses light induced stomata opening by interacting with ROP Interactive CRIB Motif Containing Protein7 (RIC7), which in turn interacts and inhibits the exocyst vesicle tethering complex subunit Exo70B1 (Hong et al. 2015). ROP2 is additionally involved in pavement cell lobe interdigitation by interacting with RIC4 for actin assembly in lobes and at the same time inhibiting RIC1 which is known to organize microtubules together with the katanin KTN1 and ROP6 (Fu et al. 2005, Lin et al. 2013). In these pathways, RIC proteins are considered as scaffolds for connecting activated ROPs with downstream effector proteins in G-protein signaling.

Another class of downstream interactors are ROP Interactive Partners (RIPs, alternatively called Interactor of Constitutive Active ROP, ICR). RIPs represent a second class of plant-specific proteins connecting ROP signaling to downstream effectors. So far, very little is known about these proteins. Arabidopsis knockout plants of RIP1/ICR1 have defects in pavement cell development, root hair development as well as root meristem maintenance showing an involvement of RIP1/ICR1 in different developmental processes. RIP1/ICR1 seems to be able to interact with different ROP proteins and was found to interact downstream with SEC3a of the exocyst complex and thereby possibly controlling the localization of the auxin transporter PIN1 (Lavy et al. 2007, Hazak et al. 2010, Hazak et al. 2014). Additionally it was reported, that RIP1 acts in pollen tube formation where it interacts with ROP1 at the plasma membrane of the pollen tube tip (Li et al. 2008). RIP3 (also called ICR5 or MIDD1 for Microtubule Depletion Domain1) plays a key role in xylem cell development in Arabidopsis. During the formation of the secondary cell wall in progenitor cells, RIP3 interacts with ROP11 and the kinesin KIN13A, which leads to local microtubule

depletion and the formation of secondary wall pits (Mucha et al. 2010, Oda et al. 2010, Oda and Fukuda 2012, Oda and Fukuda 2013).

ROP GTPases also play a role as signaling components in plant defense (Ono et al. 2001, Chen et al. 2010). For instance, upon chitin perception, the receptor kinase CERK1 phosphorylates RacGEF1, a ROP guanosine nucleotide exchange factor that in turn activates RAC1, which supports immunity to *Magnaporthe oryzae* (Akamatsu et al. 2013).

The barley ROP protein RACB is involved in root hair outgrowth and controls asymmetric cell division of subsidiary cells in stomata development (Scheler et al. 2016). RACB and RACB-associated proteins influence arrays and stability of filamentous actin and the microtubule cytoskeleton (Opalski et al. 2005, Hoefle et al. 2011, Huesmann et al. 2012). Next to its function in polar cell development, RACB is also a susceptibility factor in the interaction with the powdery mildew fungus *Bgh*. Over-expression of constitutively activated RACB (CA RACB) enhances the penetration success of *Bgh* into barley epidermal cells, silencing of RACB leads to a decreased penetration rate (Schultheiss et al. 2002, Schultheiss et al. 2003, Hoefle et al. 2011). RACB's function in susceptibility seems not to be dependent on defense suppression, but rather on the exploitation of developmental signaling mechanisms of the host (Scheler et al. 2016). A retrotransposon encoded *Bgh* effector candidate, ROP-Interactive Peptide1 (ROPIP1), binds directly to activated RACB. Expression of ROPIP1 in barley cells negatively influences microtubule stability and leads to an increased penetration rate of *Bgh* into barley epidermal cells (Nottensteiner et al. 2018). RACB further interacts with the class VI receptor-like cytoplasmic kinase ROP-Binding Kinase1 (RBK1). Activated RACB supports kinase activity of RBK1, but RBK1 acts in resistance rather than susceptibility. This seems to be explained by the interaction of RBK1 with S-Phase Kinase1-Associated (SKP1)-Like Protein (SKP1-like), which is part of an E3-ubiquitin ligase complex and both RBK1 and SKP1-like can limit the abundance of the RACB protein (Huesmann et al. 2012, Reiner et al. 2015). Another interactor of RACB is the Microtubule-Associated ROP GTPase Activating Protein1 (MAGAP1), a CRIB-motif containing ROP-GAP that may have the potential to switch off RACB. MAGAP1 and RACB recruit each other to the cell

periphery and to the microtubule cytoskeleton, and MAGAP1 apparently counters the susceptibility effect of RACB, while silencing of MAGAP1 leads to increased susceptibility to *Bgh* (Hoefle et al. 2011).

In this study, we identified barley RIPb as another downstream interactor of RACB. We investigated the effect of RIPb on susceptibility by transient over-expression and RNAi knockdown of RIPb in single epidermal cells, and the interaction between RIPb and RACB by Yeast-Two-Hybrid assays and ratiometric bimolecular fluorescence complementation (BiFC). RIPb and RACB co-localize and presumably interact at the plasma membrane, at the microtubule cytoskeleton, and at the site of fungal invasion. To further investigate the structure-function relationship of RIPb, we tested a series of RIPb truncations regarding their function in the interaction of barley with *Bgh* and their role for protein-protein interaction.

Results

Identification of RIP proteins in barley

Previous studies have shown that RIP proteins are a class of proteins with very little sequence similarity (Li et al. 2008). All RIP proteins identified so far in Arabidopsis contain an N-terminal QEEL motif and a C-terminal QWRKAA motif. These motifs are present in respective N- and C-terminal coiled-coil domains. Based on this, we performed bioinformatic analyses and identified three high confidence genes coding for RIP proteins in barley (Fig. 1). It appears that in several monocots the first glutamic acid in the QEEL motif is exchanged to aspartic acid (QDEL). We named these proteins RIPa (HORVU3Hr1G087430), RIPb (HORVU1Hr1G012460) and RIPc (HORVU3Hr1G072880), since we did not observe a clear orthology to individual Arabidopsis RIP proteins and phylogenetic analysis was ambiguous as well (Fig. 1B). We also identified three RIP proteins in rice containing the QDEL motif as well as the QWRKAA motif (Os01g61760, Os05g03120 and OsJ_03509 (Yu et al. 2005)). Alignments of the barley RIPs with the RIP proteins from rice and the five RIP proteins previously identified in Arabidopsis (RIP1/ICR1 (At1g17140), RIP2/ICR2 (At2g37080),

RIP3/MIDD1 (At3g53350), RIP4 (At1g78430) and RIP5 (At5g60210)) show little overall amino acid sequence conservation between the grasses and Arabidopsis, except for the conserved QD/EEL motif at the N-terminus and the QWRKAA motif at the C-terminus. The latter was shown to be necessary for ROP interaction (Lavy et al. 2007). The alignment also shows conservation of lysine residues at the very C-termini, which were shown before to be important for membrane localization of other RIP proteins (Li et al. 2008) (Fig. 1A).

Phylogenetic analysis shows that HvRIPa and HvRIPb are more closely related to each other, than HvRIPc, which is located on an independent branch of the tree (Fig. 1B). Two RIPs from rice (*Oryza sativa* ssp. *japonica*) and two RIPs from *Brachypodium distachyon* (BRADI_2g54177v3, BRADI2g37920v3) seem to be orthologous to HvRIPa and HvRIPb. Both rice and *B. distachyon* also encode a putative ortholog of HvRIPc (BRADI_2g50317v3). HvRIPc, AtRIP1 and AtRIP4 share a similar C-terminus with a KKGN/QK motif and AtRIP1 and AtRIP4 also share one branch with HvRIPc on the phylogenetic tree.

RIPb influences susceptibility of barley to *Bgh*

Semiquantitative reverse transcription PCR shows that all three barley RIPs are transcribed in the epidermis, with RIPb showing the highest RNA levels. Samples from inoculated leaves show no increase in transcription levels of any of the three barley *RIPs* (Supplemental Fig. S1).

To investigate, if one of the RIPs influences susceptibility of barley to *Bgh,* we tested the penetration efficiency of *Bgh* into transiently transformed epidermal cells. We introduced either an over-expressing construct under control of the CaMV35S promotor or a posttranscriptional gene-silencing construct into these cells. Over-expression of RIPa or RIPc had no significant effect on susceptibility (Supplemental Fig. 4A). Over-expression of RIPb however, significantly and consistently increased the penetration rate of *Bgh* into transformed cells by about 22%, compared to cells transformed with the empty vector control (Fig. 2A). RNA interference (RNAi)-mediated silencing of RIPb, did not significantly change the penetration rate of *Bgh* into the transformed cells (Fig. 2B).

RIPb interacts with RACB

In order to ascertain the subcellular localization of RIPb, we transiently expressed an YFP-tagged fusion protein of RIPb in single epidermal cells via biolistic transformation. Co-expression with the barley microtubule marker RFP-MAGAP1-Cter (Hoefle et al. 2011) showed partial co-localization of RIPb and MAGAP1-Cter at cortical microtubules (Fig. 3B, C). This was further supported by quantification of signal intensities at the periclinal cell periphery, which showed that YFP-RIPb signals peaked at the same sites as the microtubule marker but also showed background signals (Fig. 3C). This further suggested that YFP-RIPb is also present in the cytosol and in the cell periphery or plasma membrane. Co-expression with either constitutively activated RACB-G15V (CA RACB) or dominant negative RACB-T20N (DN RACB) resulted in reduced cytosolic localization of RIPb in presence of CA RACB, but not DN RACB (Fig. 4A). This change in RIPb localization might be best explained if RACB recruits RIPb to the cell periphery/plasma membrane. Co-expression experiments with YFP-RIPbCC1Va truncation lacking the predicted ROP interactive CC2 domain (see below, Fig. 5) and CA RACB shows that YFP-RIPbCC1Va could not the relocated to the cell periphery by CA RACB (Supplemental Fig. S3), suggesting that the CC2 domain is necessary for the recruitment by RACB. Ratiometric Bimolecular Fluorescence Complementation (BiFC) experiments further supported the interaction of RIPb with RACB. YFP fluorescence was reconstituted when nYFP-RIPb and cYFP-CA RACB were co-expressed in leaf epidermal cells (Fig. 4B, C). By contrast, co-expression of nYFP-RIPb and cYFP-DN RACB did not result in clear BiFC and the strength in signals were in average only about 10% of the signals recorded for the interaction with CA RACB (Fig. 4B, C). We observed the complemented CA RACB-RIPb YFP complex signals either exclusively at the plasma membrane or at cortical microtubules and the plasma membrane (Fig. 4B). We further confirmed a direct interaction between both wild type RACB (RACB WT) and CA RACB with RIPb (Fig 4D), respectively, in yeast. These experiments together suggest a direct interaction between RIPb and RACB *in planta*.

RIPb truncations show distinct subcellular localization and function

All predicted RIP proteins from *H. vulgare*, *O. sativa*, *A. thaliana* and *B. distachyon* contain an N-terminal coiled-coil-(CC) domain with the QD/EEL motif as well as a C-terminal CC-domain containing the QWRKAA motif (Fig. 1A; Fig. 5A). Based on this and with regard to previous studies (Mucha et al. 2010), we created truncated constructs of RIPb to further assess the roles of the individual protein domains. We split the protein into three fragments either containing or not the first CC-domain (CC1), the central variable region (Va) and the second CC-domain (CC2). In yeast, only constructs containing the CC2 domain and hence the QWRKAA motif interacted with CA RACB as it was shown before for the interaction of Arabidopsis ROPs and RIPs (Fig. 5C) (Lavy et al. 2007, Mucha et al. 2010). BiFC experiments indicated that the interaction between RIPbCC2 and RACB takes place at the cell periphery. RIPbCC2 was able to interact with CA RACB, not with DN RACB (Supplemental Fig. S2). RIPb was also able to interact with itself in yeast. Amino acids important for this must be located in the Va-region, since only full length RIPb and truncations containing this region were able to interact in yeast (Fig. 5D). In order to look for specific subcellular localizations *in planta*, we created YFP-tagged fusion proteins of these truncations. YFP-RIPbCC2 and YFP-RIPbVaCC2 localize strongly to the cell periphery, presumably the plasma membrane (Fig. 5B). YFP-RIPbCC1Va was located in the cytosol and at the microtubules. However, YFP-RIPbCC1 and RIPbVa were detected in the cytosol only (Fig. 5B). Hence, both the CC1 domain and the Va domain appeared to be required but not sufficient for microtubule association. Double mutation of D85 and E86 of the QDEL motif did not lead to a loss of microtubule localization (Supplemental Fig. S3b). The QDEL motif itself might therefore not be necessary for microtubule localization. Since the Va domain is also required for dimerization, RIPb might localize to the microtubules rather as a dimer or oligomer than as a monomer. This was further supported because BiFC-signals recorded after co-expression of nYFP-RIPb with cYFP-RIPb occur exclusively at the microtubules and show less cytosolic background, when compared to YFP-RIPb alone, which may be detectable, both in its

monomeric and its dimeric/oligomeric form (Fig. 6A, C). Signal analysis showed high signal overlay between the complemented YFP signal and microtubule marker RFP-MAGAP1-Cter over a linear region of interest (Fig. 6C, D). Quantification of complemented YFP signals showed significantly stronger signal between nYFP-RIPb and cYFP-RIPb compared to the co-expression of the microtubule-localized nYFP-MAGAP1 and cYFP-RIPb. nYFP-MAGAP1 on the other hand showed YFP complementation when co-expressed with cYFP-CA RACB (Fig. 6A, B).

Results from Lavy et al. (2007) and Mucha et al. (2010) suggest, that RIPs lacking a functional QWRKAA motif, lose the ability to interact with ROPs and that either CC1 or CC2 domains bind to further downstream signaling components. This indicates that RIPb might be able to fulfill a ROP signaling function through one of these domains. To test the functionality of RIPb truncations, we tested their effect on penetration success of *Bgh* on barley. Interestingly over-expression of RIPbCC2 (Fig. 2C) strongly increased susceptibility by about 75%. In contrast, over-expression of the CC2-domain of RIPa did not lead to a significant increase in susceptibility (Supplemental Fig. S4B). The effect of RIPbCC2 completely disappeared when we expressed the longer RIPbVaCC2 construct, containing additionally the Va-domain. The CC1-domain alone also increased susceptibility by about 35% and this effect was also reduced when we expressed the longer RIPbCC1Va truncation (Fig. 2C). This indicated a possible regulatory function of the Va domain of RIPb.

RACB and RIPb co-localize at the site of fungal attack

Since RIPb and RACB can interact *in planta* and both proteins can influence susceptibility, we wanted to know whether RIPb and RACB would co-localize at the sites of fungal penetration. Therefore, we transiently co-expressed YFP-RIPb and CFP-RACB in single epidermal cells and inoculated the leaves with conidia of *Bgh*. At 24 h after inoculation, we observed ring-like accumulations of both YFP-RIPb and CFP-RACB at the site of fungal penetration around the haustorial neck. Cytosolic mCherry appeared less spatially confined (Fig. 7A). We observed even more pronounced fluorescence at infection sites, when YFP-tagged RIPb was co-expressed

297 with CA RACB. In this context, we detected clear accumulation of RIPb and
298 CA RACB at the site of fungal penetration, though independent of the
299 outcome of the penetration attempt. If the penetration was successful, a
300 clear ring-like localization pattern around the haustorial neck could be
301 observed. However, if the fungal penetration was not successful we
302 detected a more fringed accumulation of both proteins, possibly
303 representing membrane domains around papilla protrusions (Fig. 7B). Since
304 RIPbCC2 had a stronger influence on fungal penetration success than full
305 length RIPb, we also imaged YFP-RIPbCC2 when co-expressed with CFP-
306 CA RACB. Interestingly, there was a very strong co-localization of both
307 proteins around the haustorial neck region in penetrated cells, but also in
308 some instances at sites of repelled fungal attempts (Fig. 7C). The ring-like
309 accumulation of RIPbCC2 around the haustorial neck was also visible at
310 later stages of the interaction at 48 hours after the inoculation (Fig. 7D).
311 There was also constantly local aggregation of cytoplasm at the sites of
312 attack, but measurements of the ring-like YFP-RIPbCC2 fluorescence,
313 showed signal intensities were clearly more confined to the cell periphery
314 compared to cytosolic mCherry fluorescence (Fig. 7E).
315
316

317 ## Discussion

318 RIP proteins are considered scaffold proteins in ROP signaling. Next to
319 RICs, RIPs might be key factors in diversification of G-protein signaling in
320 plants. It appears that so far most described downstream interactions of
321 ROPs are mediated through either RIC or RIP proteins. All RIPs contain the
322 characteristic QWRKAA motif in the CC2 domain, which was previously
323 described as the motif responsible for ROP interaction (Lavy et al. 2007).
324 Our results support this, since only full length RIPb and truncations
325 containing this motif interacted with RACB and were subcellularly recruited
326 by CA RACB. (Fig. 4, Fig. 5, Supplemantal Fig. S2). The CC2 domain is part
327 of all predicted RIPs form *A. thaliana*, *O. sativa*, *B. distachyion* and *H.*
328 *vulgare*. All identified RIPs from these four species also contain a conserved
329 QD/EEL motif located in an N-terminal CC1 domain (Fig. 1). The function of

this motif, however, remains more elusive. Although the CC1 domain is important for microtubule localization of RIPb (Fig. 5), amino acid exchanges in the QDEL motif did not result a loss of microtubule association (Supplemantal Fig. S3).

Phylogenetic analyses show that both rice and Brachypodium, possess putative orthologs of each of the three barley RIPs, implying possible conserved function of the RIPs in grasses (Fig. 1). However, the five RIP proteins of Arabidopsis show no clear phylogenetic relation to the grass RIPs. It would be interesting to see, whether Arabidopsis and monocot RIPs have similar functions, or may have evolved in different directions as the little sequence conservation suggests.

For this study, we focused on a possible RACB signaling mechanism via RIP proteins during the interaction of barley and *Bgh*. Barley RIPb interacts with CA and wild type RACB in yeast, supporting that it is a potential downstream interactor of RACB. Over-expression of RIPb but not RIPa and RIPc increased penetration rate of *Bgh* into transformed epidermal barley cells (Fig. 2, Supplemental Fig. S4A). Together with the fact that the RIPb transcript was more abundant in the epidermis of barley than RIPa or RIPc transcripts, this might indicate that RIPb is the only barley RIP with a possible function in powdery mildew interaction, although RIPb silencing had no significant effect on the interaction between epidermal cells and *Bgh* (Fig. 2B). This might be due to branching of RACB downstream signaling which could compensate for the lack of RIPb during the interaction. For instance RIC171 might act as an alternative downstream interactor of RACB (Schultheiss et al. 2008), and it is possible that even more interactors of RACB are involved, because ROP proteins are considered signaling hubs (Nibau et al. 2006). Hence silencing of only one signaling branch might not have a significant effect on the interaction, whereas over-expression could support a certain RACB downstream branch and therefore has an effect.

RIPb shows diverse subcellular localizations. Next to cytosolic localization, we observed localization at the cell periphery and at the microtubule cytoskeleton (Fig. 3). The N-terminal CC1 domain seems to be necessary but not sufficient for microtubule localization, since the RIPbVaCC2 truncation lacking the CC1-domain was not able to localize to microtubules,

but the CC1 domain alone also did not show microtubule localization. The central Va domain alone was also insufficient for microtubule association but it appeared to be required for both microtubule association and RIPb-RIPb interaction (Fig. 5D), because in contrast to RIPbCC1, RIPbCC1Va showed microtubule localization (Fig. 5B). BiFC experiments further suggested that the RIPb-RIPb interaction takes place at microtubules (Fig. 6). Interestingly, truncated versions of RIPb, which contain the Va domain, did not induce susceptibility when over-expressed, whereas RIPbCC1 and particularly RIPbCC2 induced susceptibility, similar to or much stronger than the full length protein. We therefore hypothesize that dimerization or oligomerization of RIPb at microtubules might have a regulatory purpose, potentially by sequestration of inactive RIPb.

Over-expression of the RIPbCC2 domain resulted in a very strong increase in susceptibility of barley epidermal cells to *Bgh.* Lavy et al. (2007) showed that the QWRKAA motif in the CC2 domain of Arabidopsis AtRIP1 (ICR1) is not only necessary for ROP interaction, but also for the interaction with the downstream interactor AtSEC3, indicating that the CC2 domain might be able to fulfill the signaling function of AtRIP1. This might also be the case for RIPbCC2. By contrast, over-expression of the CC2 domain of HvRIPa did not result in a significant increase in susceptibility (Supplemental Fig. S4B), and therefore this effect appears specific for RIPb. RIPbCC2 was able to interact with RACB in yeast and *in planta* (Fig. 5, Supplemental Fig. S2). Furthermore, RIPb did not localize to the cell periphery anymore without the CC2 domain (RIPbCC1Va) even in presence of CA RACB (Supplemental Fig. S3). This together suggests, that the CC2 domain of RIPb is responsible both for ROP interaction and for a downstream function, which my take place at the plasma membrane.

The N-terminal CC1 domain of RIPb is required for microtubule association but might interact with signaling components as well. This would explain the susceptibility phenotype of the CC1 domain, although the CC1 domain itself does not interact with RACB (Fig. 2C, Fig. 5C). Interestingly, the CC1 domain of Arabidopsis AtRIP3/MIDD1 is required for interaction with KINESIN13A (Mucha et al. 2010). It could hence be that RIPb fulfills a dual function via different domains of the protein.

BiFC experiments showed interaction between RACB and RIPb at the microtubules and at the plasma membrane. Since RACB alone does not localize to microtubules (Schultheiss et al. 2003) it seems that RIPb is able to recruit RACB to microtubules when over-expressed. The interaction between the susceptibility-inducing CC2 domain and RACB on the other hand takes place at the plasma membrane (Supplemental Fig. S2). These results suggest that RACB likewise recruits RIPb to the plasma membrane during susceptibility signaling and that recruitment of RACB to microtubules has rather limits this effect. We speculate that in this experimental setup, recruitment of RACB to microtubules brings RACB into proximity of microtubule-located MAGAP1, which presumably inactivates RACB (Hoefle et al. 2011). This might explain why full length RIPb has a less strong effect on susceptibility when compared to RIPbCC2, which cannot recruit RACB to the microtubules.

We observed co-localization of RIPb and RACB and of RIPbCC2 and RACB at the site of fungal attack. In interactions where the fungus was able to penetrate the host cell, a ring of RIPb and RACB or CA RACB around the haustorial neck at the plasma membrane, could be observed. However, we could also observe accumulation of signal in repelled penetration attempts around the formed papilla, indicating that accumulation of these two proteins alone is not sufficient to render all cells susceptible. RACB possesses a C-terminal CSIL motif, which is predicted to mediate protein prenylation at the cysteine residue, and is necessary for plasma membrane association and function in susceptibility (Schultheiss et al. 2003). Additionally, RACB has a polybasic stretch close to the C-terminus (Schultheiss et al. 2003) shown for other ROPs to be involved in lipid interaction (Platre et al. 2019) and a conserved cysteine at position C158, which is S-acylated in activated Arabidopsis AtROP6 (Sorek et al. 2017). Hence, lipid modification and interaction with negatively charged phospholipids together may bring activated RACB-GTP to specific membrane domains, to which it then recruits proteins that execute ROP signaling function. Phosphatidylserine and phophoinositides are often involved in defining areas of cell polarization in membranes for example during root hair and pollen tube tip growth (Helling et al. 2006, Kusano et al. 2008, Platre et al. 2019) and ROPs are

known to moderate the phosphorylation pattern of phosphoinositides during polarization (Kost et al. 1999). We hence speculate that localization of ROP signaling components at the site of interaction reflects domains of enriched negatively charged phospholipids.

The exact effect of RACB-RIPb signaling on the interaction remains unknown so far. However, the finding that Arabidopsis RIPs interact with proteins of the exocyst complex and KINESIN13A opens the possibility that barley RIPs also modify the cytoskeleton or membrane trafficking, both being key to resistance and susceptibility in powdery mildew interactions (Hückelhoven and Panstruga 2011, Dörmann et al. 2014). Together, our data support a new hypothesis according to which RIPb is inactive at microtubules and recruited to RACB signaling hotspots at the cell periphery by activated RACB-GTP. There it might interact with further proteins of the RACB signaling pathway to facilitate fungal entry into barley epidermal cells. The fact that the putative fungal effector ROPIP1 destabilizes barley microtubules (Nottensteiner et al. 2018) adds another level of complexity, on which ROPIP1 may foster release of RIPb from microtubules for its function in susceptibility.

Conclusions

Over the last years, the impact of susceptibility factors for plant – pathogen interactions has become more and more obvious. Barley RACB might be a key player in cellular polarization during fungal invasion. Here we identified RIPb as a downstream interactor of RACB in susceptibility. RACB and RIPb together might be involved in fine-tuning of cell polarization in advantage of the fungus. It will be important to identify further interactors of RIPb and in particular of its susceptibility-supporting CC2 domain. This may establish a deep understanding of the components and mechanisms of subcellular reorganizations in the cell cortex, which support the biotrophic parasite *Bgh* in accommodation of its haustorium in an intact epidermal cell.

Material and Methods

Biological Material

Barley (*Hordeum vulgare*) cultivar Golden Promise was used in all experiments. Plants were grown under long day conditions with 16h of light and 8h in the dark with a relative humidity of 65% and light intensity of 150 µM s^{-1} m^{-2} at a temperature of 18°C.

Powdery mildew fungus *Blumeria graminis* f.sp. *hordei* race A6 was cultivated on wild type Golden Promise plants under the conditions described above and inoculated by blowing spores into a plastic tent that was positioned over healthy plants or transformed leaf segments.

Cloning procedures

HvRIPb (*HORVU1Hr1G012460*) was amplified from cDNA using primers Ripb-EcoRI_fwd and Ripb-BamHI_rev (Supplemental Tab. 1) introducing EcoRI and BamHI restriction sites, respectively. *HvRIPa* (HORVU3Hr1G087430) was amplified from cDNA using primers RipaXbaI_fwd and RipaXbaI_rev introducing XbaI restriction sites at 5' and 3' ends. *HvRIPc* (HORVU3Hr1G072880) was amplified from cDNA using primers RipcXbaI_fwd and RipcPstI_rev introducing restriction sites for XbaI at the 5' end and for SalI at the 3' end. The amplified products were ligated into the pGEM-T easy vector (Promega, Madison, WI, USA) by blunt end cloning according to the manufacturer's instructions and sequenced. *HvRIPb* truncations spanning the following amino acids. *HvRIPbCC1* from amino acid 1 to 132, *HvRIPbVa* from amino acid 133 to 420 and *HvRIPbCC2* from amino acid 420 to 612. *HvRIPb* truncations for Yeast-Two-Hybrid were amplified from pGEM-T easy containing full length *RIPb* using primers with EcoRI and BamHI restriction sites. *RIPbCC1* was amplified using primers Ripb-EcoRI_fwd and RipbCC1BamHI_rev, *RIPbCC1Va* with primers Ripb-EcoRI_fwd and RipbVaBamHI_rev, *RIPbVa* with primers RipbVaEcoRI_fwd and RipbVaBamHI_rev, *RIPbVaCC2* with primers RipbVaEcoRI_fwd and Ripb-BamHI_rev and *RIPbCC2* with primers RipbC2EcoRI_fwd. Each reverse primer introduced a stop codon. For Yeast-Two-Hybrid assays *HvRIPb* and *HvRIPb* truncations were subcloned from the pGEM-T easy vector into pGADT7 and pGBKT7 plasmids (Clontech Laboratories) using the EcoRI and BamHI restriction sites. For over-expression constructs and

constructs for protein localization the pUC18-based vector pGY1, containing a CaMV35S promotor was used. (Schweizer et al. 1999). From the pGEM-T easy vector, *HvRIPb* was further amplified with primers Ripb-XbaI_fwd and Ripb-SalI_rev, containing XbaI and SalI restriction site, respectively. Using those restriction sites *HvRIPb* was then ligated into the pGY1 plasmid and pGY1-YFP plasmid for N-terminal YFP fusion. *HvRIPa* and *HvRIPc* were subcloned form pGEM-T easy into pGY1 using the XbaI restriction site for *HvRIPa* and the XbaI and PstI restriction sites for *HvRIPc*. Over-expression construct for *HvRIPaCC2* was produced by introducing attB-attachment sites for Gateway cloning. For this, a first PCR was performed with primers GW1-RipaCC2_fwd and GW1-Ripa_rev using pGEM-T easy construct as template. A subsequent second PCR was performed using primers Gate2_F and Gate2_R to introduce attB attachment sites for Gateway cloning. The construct was then cloned by BP-clonase reaction using the Gateway BP Clonase™ II (Invitrogen) into the pDONR223 entry vector (Invitrogen). From there *HvRIPaCC2* was cloned by LR-clonase reaction with Gateway LR Clonase™ II (Invitrogen) into pGY1-GW, a modified pGY1 vector containing the gateway cassette. The pGY1-GW plasmid was constructed using the Gateway™ Vector Conversion System (Invitrogen) according to the manufacturer's instructions.

For BiFC, *HvRIPb* was amplified from the pGEM-T easy vector using the primer Ripb-SpeI_fwd and Ripb-SalI_rev with restriction sites for SpeI and SalI, respectively. The construct was then digested with SpeI and SalI and ligated into pUC-SPYNE(R)173 and pUC-SPYCE(MR) plasmid (Waadt et al. 2008) using these restriction sites.

A 538bp long RNAi sequence for *HvRIPb* was amplified, using primers RipbRNAi_fwd and RipbRNAi_rev, and introduced into the pIPKTA38 vector by blunt-end cloning using the SmaI restriction site (Douchkov et al. 2005). This plasmid was used as entry vector to clone the RNAi Sequence into the pIPKTA30N vector for double-strand RNA formation via Gateway LR Clonase™ II (Invitrogen) reaction according to the manufacturer's instruction.

All *HvRIPb* truncations were introduced into the pGY1-YFP plasmid for N-terminal YFP fusion using the following primer. For *HvRIPbCC1* primer Ripb-

XbaI_fwd and RipbC1-SalI_rev, for *HvRIPbCC1Va* primer Ripb-XbaI_fwd and RipbVa-SalI_rev, for *HvRIPbVa* primer RipbVa-XbaI_fwd and RipbVa-SalI_rev, for *HvRIPbVaCC2* primer RipbVa-XbaI_fwd and Ripb-SalI_rev and for *HvRIPbCC2* primer RipbC2-XbaI_fwd and Ripb-SalI_rev. All forward primers introduce a XbaI restriction site and all reverse primer contain a SalI restriction site, which were used for the ligation into pGY1-YFP. The same products and restriction sites were used for ligation into the pGY1 vector except for *HvRIPbCC1Va*. For *HvRIPbCC1Va* primer GW-Ripb_fwd and GW1-RipbC1Va_rev was used for amplification followed by a second PCR with primers Gate2_F and Gate2_R to introduce attB attachment sites for Gateway cloning. The construct was then cloned by BP-clonase reaction using the Gateway BP Clonase™ II (Invitrogen) into the pDONR223 entry vector (Invitrogen). From there *HvRIPbCC1Va* was cloned by LR-clonase reaction with Gateway LR Clonase™ II (Invitrogen) into pGY1-GW.

Transient transformation of barley cells

Barley epidermal cells were transiently transformed by biolistic particle bombardment using the PDS-1000/HE (Biorad, Hercules, CA; USA). For this 7d old primary leaves of barley were cut and placed on 0.8% water-agar. Per shot 302.5µg of 1µm gold particles (Biorad, Hercules, CA, USA) were coated with 1µg plasmid per shot. 0.5µg plasmid per shot was used for cytosolic transformation markers. After addition of plasmids to the gold particles, $CaCl_2$ was added to a final concentration of 0.5M. Finally, 3µl of 2mg/ml Protamine (Sigma) were added to the mixture per shot. After incubation for half an hour at room temperature, gold particles were washed twice with 500µl ethanol. In the first step with 70% ethanol and in the second step with 100% ethanol. After washing, the gold particles were re-suspended in 6µl of 100% ethanol per shot and placed on the macro carrier for bombardment.

Alignments and Phylogenetic Analysis

Sequences of Arabidopsis RIP proteins were used to identify barley RIPs using the IPK Barley BLAST Server (https://webblast.ipk-gatersleben.de/barley_ibsc/viroblast.php). RIPs from *Oryza sativa spp.*

Japonica were identified using the BLAST tool on the Rice Genome Annotation Project (http://rice.plantbiology.msu.edu/home_faq.shtml (Kawahara et al. 2013)). RIPs from *Brachypodium distachyon* were identified by BLAST search on EnsemblPLANTs (https://plants.ensembl.org/index.html). The Alignment of RIP protein sequences was done with ClustalO (https://www.ebi.ac.uk/Tools/msa/clustalo/) and displayed with Jalview (jalview 2.10.5). A phylogenetic maximum likelihood tree was generated, using the PhyML tool in the program seaview (v4.7).

Determination of Susceptibility

Transiently transformed barley leaves were inoculated with *Bgh* 24 h after bombardment for over-expression constructs and 48 h after bombardment for gene silencing constructs. 24 h after inoculation penetration rate into the transformed cells was determined by fluorescence microscopy as described before (Hückelhoven et al. 2003).

Protein localization and Protein – Protein Interaction *in planta*

Localization of HvRIPb and co-localization of HvRIPb and HvRACB were determined by transiently transforming barley epidermal cells with plasmids encoding fluorophore fusion proteins. Imaging was done with a Leica TCS SP5 microscope equipped with hybrid HyD detectors. CFP was excited at 458nm and detected between 465nm and 500nm. YFP was excited at 514nm and detected between 525nm and 500nm. Excitation of mCherry and RFP was done at 561nm and detection between 570nm and 610nm.

For ratiometric quantification of BiFC experiments Mean Fluorescence Intensity (MFI) was measured over a region of interest at the cell periphery. Background signal was subtracted and ratio between YFP and mCherry signal was calculated. At least 25 cells were analyzed per construct for each experiment. Images were taken 24 hours to 48 hours after transformation by particle bombardment.

Yeast Two-Hybrid assays

For targeted yeast two-hybrid assays, *HvRIPb* and its truncations were introduced into pGADT7. Introduction of *HvRACB* into pGBKT7 was described in Schultheiss et al. (2008). Constructs were transformed into yeast strain AH109 following the small-scale LiAc yeast transformation procedure from the Yeast Protocol Handbook (Clontech, Mountain View, CA, USA).

RNA extraction and semiquantitative PCR (qRT-PCR)

RNA was extracted from barley tissue using the TRIzolTM-Reagent by Invitrogen according to the manufacturer's instructions. 1µg of RNA was reverse transcribed with the QuantiTect Reverse Transcription Kit (Qiagen, Hilden, Germany) according to the manufacturer's instructions.

For semiquantitative PCR, 2µl of cDNA transcribed from RNA of pealed epidermis from barley leaves, were used. Samples were taken from leaves 24h after inoculation with *Bgh*, or from uninoculated leaves of the same age. A 209bp fragment of *RIPa* was amplified with an annealing temperature (T_a) of 58°C with primers Ripa_sqPCR4_fwd and Ripa_sqPCR5_rev (Supplemantal Tab1). For *RIPb* a 181bp fragment was amplified with a T_a of 56°C using primers Ripb_sqPCR9_fwd and RIPb_sqPCR10_rev. For *RIPc* a 168bp fragment was amplified at T_a 58°C using primers Ripc_sqPCR4_fwd and Ripc_sqPCR5_rev. As control *HvUbc* was amplified at T_a 61°C using primers HvUBC2_fwd and HvUBC2_rev (Ovesna et al. 2012).

Acknowledgments

The project was funded in frame of research grants from the German Research Foundation to RH (DFG HU886-8 and SFB924).

626

627 **References**

628 Akamatsu, A., H. L. Wong, M. Fujiwara, J. Okuda, K. Nishide, K. Uno, K.
629 Imai, K. Umemura, T. Kawasaki, Y. Kawano and K. Shimamoto (2013).
630 "An OsCEBiP/OsCERK1-OsRacGEF1-OsRac1 module is an essential
631 early component of chitin-induced rice immunity." Cell Host Microbe
632 **13**(4): 465-476.
633 Catanzariti, A. M., P. N. Dodds and J. G. Ellis (2007). "Avirulence proteins
634 from haustoria-forming pathogens." FEMS Microbiol Lett **269**(2): 181-
635 188.
636 Chen, L., K. Shiotani, T. Togashi, D. Miki, M. Aoyama, H. L. Wong, T.
637 Kawasaki and K. Shimamoto (2010). "Analysis of the Rac/Rop small
638 GTPase family in rice: expression, subcellular localization and role in
639 disease resistance." Plant Cell Physiol **51**(4): 585-595.
640 Chowdhury, J., M. Henderson, P. Schweizer, R. A. Burton, G. B. Fincher
641 and A. Little (2014). "Differential accumulation of callose,
642 arabinoxylan and cellulose in nonpenetrated versus penetrated
643 papillae on leaves of barley infected with Blumeria graminis f. sp.
644 hordei." New Phytol **204**(3): 650-660.
645 Dörmann, P., H. Kim, T. Ott, P. Schulze-Lefert, M. Trujillo, V. Wewer and R.
646 Hückelhoven (2014). "Cell-autonomous defense, re-organization and
647 trafficking of membranes in plant-microbe interactions." New
648 Phytologist **204**(4): 815-822.
649 Douchkov, D., D. Nowara, U. Zierold and P. Schweizer (2005). "A high-
650 throughput gene-silencing system for the functional assessment of
651 defense-related genes in barley epidermal cells." Molecular Plant-
652 Microbe Interactions **18**(8): 755-761.
653 Feiguelman, G., Y. Fu and S. Yalovsky (2018). "ROP GTPases Structure-
654 Function and Signaling Pathways." Plant Physiol **176**(1): 57-79.
655 Fu, Y., Y. Gu, Z. Zheng, G. Wasteneys and Z. Yang (2005). "Arabidopsis
656 interdigitating cell growth requires two antagonistic pathways with
657 opposing action on cell morphogenesis." Cell **120**(5): 687-700.
658 Fuchs, R., M. Kopischke, C. Klapprodt, G. Hause, A. J. Meyer, M.
659 Schwarzlander, M. D. Fricker and V. Lipka (2016). "Immobilized

660 Subpopulations of Leaf Epidermal Mitochondria Mediate
661 PENETRATION2-Dependent Pathogen Entry Control in Arabidopsis."
662 Plant Cell **28**(1): 130-145.
663 Gross, P., C. Julius, E. Schmelzer and K. Hahlbrock (1993). "Translocation
664 of cytoplasm and nucleus to fungal penetration sites is associated with
665 depolymerization of microtubules and defence gene activation in
666 infected, cultured parsley cells." EMBO J **12**(5): 1735-1744.
667 Hahn, M., U. Neef, C. Struck, M. Gottfert and K. Mendgen (1997). "A putative
668 amino acid transporter is specifically expressed in haustoria of the
669 rust fungus Uromyces fabae." Mol Plant Microbe Interact **10**(4): 438-
670 445.
671 Hazak, O., D. Bloch, L. Poraty, H. Sternberg, J. Zhang, J. Friml and S.
672 Yalovsky (2010). "A Rho Scaffold Integrates the Secretory System
673 with Feedback Mechanisms in Regulation of Auxin Distribution." Plos
674 Biology **8**(1).
675 Hazak, O., U. Obolski, T. Prat, J. Friml, L. Hadany and S. Yalovsky (2014).
676 "Bimodal regulation of ICR1 levels generates self-organizing auxin
677 distribution." Proc Natl Acad Sci U S A **111**(50): E5471-5479.
678 Helling, D., A. Possart, S. Cottier, U. Klahre and B. Kost (2006). "Pollen
679 tube tip growth depends on plasma membrane polarization mediated
680 by tobacco PLC3 activity and endocytic membrane recycling." Plant
681 Cell **18**(12): 3519-3534.
682 Hoefle, C., C. Huesmann, H. Schultheiss, F. Bornke, G. Hensel, J. Kumlehn
683 and R. Hückelhoven (2011). "A Barley ROP GTPase ACTIVATING
684 PROTEIN Associates with Microtubules and Regulates Entry of the
685 Barley Powdery Mildew Fungus into Leaf Epidermal Cells." Plant Cell
686 **23**(6): 2422-2439.
687 Hong, D., B. W. Jeon, S. Y. Kim, J. U. Hwang and Y. Lee (2015). "The ROP2-
688 RIC7 pathway negatively regulates light-induced stomatal opening by
689 inhibiting exocyst subunit Exo70B1 in Arabidopsis." New Phytol.
690 Hückelhoven, R. (2007). "Cell wall-associated mechanisms of disease
691 resistance and susceptibility." Annu Rev Phytopathol **45**: 101-127.
692 Hückelhoven, R., C. Dechert and K. H. Kogel (2003). "Overexpression of
693 barley BAX inhibitor 1 induces breakdown of mlo-mediated penetration

694 resistance to Blumeria graminis." Proc Natl Acad Sci U S A **100**(9):
695 5555-5560.
696 Hückelhoven, R. and R. Panstruga (2011). "Cell biology of the plant-
697 powdery mildew interaction." Current Opinion in Plant Biology **14**(6):
698 738-746.
699 Huesmann, C., T. Reiner, C. Hoefle, J. Preuss, M. E. Jurca, M. Domoki, A.
700 Feher and R. Hückelhoven (2012). "Barley ROP binding kinase1 is
701 involved in microtubule organization and in basal penetration
702 resistance to the barley powdery mildew fungus." Plant Physiol **159**(1):
703 311-320.
704 Kawahara, Y., M. de la Bastide, J. P. Hamilton, H. Kanamori, W. R.
705 McCombie, S. Ouyang, D. C. Schwartz, T. Tanaka, J. Wu, S. Zhou, K.
706 L. Childs, R. M. Davidson, H. Lin, L. Quesada-Ocampo, B.
707 Vaillancourt, H. Sakai, S. S. Lee, J. Kim, H. Numa, T. Itoh, C. R. Buell
708 and T. Matsumoto (2013). "Improvement of the Oryza sativa
709 Nipponbare reference genome using next generation sequence and
710 optical map data." Rice (N Y) **6**(1): 4.
711 Kobayashi, Y., I. Kobayashi, Y. Funaki, S. Fujimoto, T. Takemoto and H.
712 Kunoh (1997). "Dynamic reorganization of microfilaments and
713 microtubules is necessary for the expression of non-host resistance in
714 barley coleoptile cells." Plant Journal **11**(3): 525-537.
715 Koh, S., A. Andre, H. Edwards, D. Ehrhardt and S. Somerville (2005).
716 "Arabidopsis thaliana subcellular responses to compatible Erysiphe
717 cichoracearum infections." Plant J **44**(3): 516-529.
718 Kost, B., E. Lemichez, P. Spielhofer, Y. Hong, K. Tolias, C. Carpenter and
719 N. H. Chua (1999). "Rac homologues and compartmentalized
720 phosphatidylinositol 4, 5-bisphosphate act in a common pathway to
721 regulate polar pollen tube growth." J Cell Biol **145**(2): 317-330.
722 Kusano, H., C. Testerink, J. E. Vermeer, T. Tsuge, H. Shimada, A. Oka, T.
723 Munnik and T. Aoyama (2008). "The Arabidopsis Phosphatidylinositol
724 Phosphate 5-Kinase PIP5K3 is a key regulator of root hair tip growth."
725 Plant Cell **20**(2): 367-380.
726 Kwaaitaal, M., M. E. Nielsen, H. Bohlenius and H. Thordal-Christensen
727 (2017). "The plant membrane surrounding powdery mildew haustoria

728 shares properties with the endoplasmic reticulum membrane." J Exp
729 Bot. 68: 5731-5743.
730 Lavy, M., D. Bloch, O. Hazak, I. Gutman, L. Poraty, N. Sorek, H. Sternberg
731 and S. Yalovsky (2007). "A Novel ROP/RAC effector links cell polarity,
732 root-meristem maintenance, and vesicle trafficking." Curr Biol **17**(11):
733 947-952.
734 Li, S., Y. Gu, A. Yan, E. Lord and Z. B. Yang (2008). "RIP1 (ROP Interactive
735 Partner 1)/ICR1 marks pollen germination sites and may act in the
736 ROP1 pathway in the control of polarized pollen growth." Mol Plant
737 **1**(6): 1021-1035.
738 Lin, D., L. Cao, Z. Zhou, L. Zhu, D. Ehrhardt, Z. Yang and Y. Fu (2013).
739 "Rho GTPase signaling activates microtubule severing to promote
740 microtubule ordering in Arabidopsis." Curr Biol **23**(4): 290-297.
741 McLusky, S. R., M. H. Bennett, M. H. Beale, M. J. Lewis, P. Gaskin and J.
742 W. Mansfield (1999). "Cell wall alterations and localized accumulation
743 of feruloyl-3 '-methoxytyramine in onion epidermis at sites of
744 attempted penetration by Botrytis allii are associated with actin
745 polarisation, peroxidase activity and suppression of flavonoid
746 biosynthesis." Plant Journal **17**(5): 523-534.
747 Mucha, E., C. Hoefle, R. Hückelhoven and A. Berken (2010). "RIP3 and
748 AtKinesin-13A-A novel interaction linking Rho proteins of plants to
749 microtubules." European Journal of Cell Biology **89**(12): 906-916.
750 Nibau, C., H. M. Wu and A. Y. Cheung (2006). "RAC/ROP GTPases: 'hubs'
751 for signal integration and diversification in plants." Trends Plant Sci
752 **11**(6): 309-315.
753 Nottensteiner, M., B. Zechmann, C. McCollum and R. Hückelhoven (2018).
754 "A barley powdery mildew fungus non-autonomous retrotransposon
755 encodes a peptide that supports penetration success on barley." J Exp
756 Bot **69**(15): 3745-3758.
757 Oda, Y. and H. Fukuda (2012). "Initiation of Cell Wall Pattern by a Rho- and
758 Microtubule-Driven Symmetry Breaking." Science **337**(6100): 1333-
759 1336.

760 Oda, Y. and H. Fukuda (2013). "Rho of plant GTPase signaling regulates
761 the behavior of Arabidopsis kinesin-13A to establish secondary cell
762 wall patterns." Plant Cell **25**(11): 4439-4450.
763 Oda, Y., Y. Iida, Y. Kondo and H. Fukuda (2010). "Wood Cell-Wall Structure
764 Requires Local 2D-Microtubule Disassembly by a Novel Plasma
765 Membrane-Anchored Protein." Current Biology **20**(13): 1197-1202.
766 Ono, E., H. L. Wong, T. Kawasaki, M. Hasegawa, O. Kodama and K.
767 Shimamoto (2001). "Essential role of the small GTPase Rac in disease
768 resistance of rice." Proc Natl Acad Sci U S A **98**(2): 759-764.
769 Opalski, K. S., H. Schultheiss, K. H. Kogel and R. Hückelhoven (2005). "The
770 receptor-like MLO protein and the RAC/ROP family G-protein RACB
771 modulate actin reorganization in barley attacked by the biotrophic
772 powdery mildew fungus Blumeria graminis f.sp. hordei." Plant J **41**(2):
773 291-303.
774 Ovesna, J., L. Kucera, K. Vaculova, K. Strymplova, I. Svobodova and L.
775 Milella (2012). "Validation of the beta-amy1 transcription profiling
776 assay and selection of reference genes suited for a RT-qPCR assay
777 in developing barley caryopsis." PLoS One **7**(7): e41886.
778 Platre, M. P., V. Bayle, L. Armengot, J. Bareille, M. D. M. Marques-Bueno,
779 A. Creff, L. Maneta-Peyret, J. B. Fiche, M. Nollmann, C. Miege, P.
780 Moreau, A. Martiniere and Y. Jaillais (2019). "Developmental control
781 of plant Rho GTPase nano-organization by the lipid
782 phosphatidylserine." Science **364**(6435): 57-62.
783 Reiner, T., C. Hoefle and R. Hückelhoven (2015). "A barley SKP1-like
784 protein controls abundance of the susceptibility factor RACB and
785 influences the interaction of barley with the barley powdery mildew
786 fungus." Mol Plant Pathol.17:184-195.
787 Scheler, B., V. Schnepf, C. Galgenmuller, S. Ranf and R. Hückelhoven
788 (2016). "Barley disease susceptibility factor RACB acts in epidermal
789 cell polarity and positioning of the nucleus." Journal of Experimental
790 Botany **67**(11): 3263-3275.
791 Schultheiss, H., C. Dechert, K. H. Kogel and R. Hückelhoven (2002). "A
792 small GTP-binding host protein is required for entry of powdery mildew

fungus into epidermal cells of barley." Plant Physiol **128**(4): 1447-1454.

Schultheiss, H., C. Dechert, K. H. Kogel and R. Hückelhoven (2003). "Functional analysis of barley RAC/ROP G-protein family members in susceptibility to the powdery mildew fungus." Plant Journal **36**(5): 589-601.

Schultheiss, H., J. Preuss, T. Pircher, R. Eichmann and R. Hückelhoven (2008). "Barley RIC171 interacts with RACB in planta and supports entry of the powdery mildew fungus." Cell Microbiol **10**(9): 1815-1826.

Schweizer, P., A. Christoffel and R. Dudler (1999). "Transient expression of members of the germin-like gene family in epidermal cells of wheat confers disease resistance." Plant J **20**(5): 541-552.

Sorek, N., L. Poraty, H. Sternberg, E. Buriakovsky, E. Bar, E. Lewinsohn and S. Yalovsky (2017). "Corrected and Republished from: Activation Status-Coupled Transient S-Acylation Determines Membrane Partitioning of a Plant Rho-Related GTPase." Mol Cell Biol **37**(23). 37(23): e00333-17

Takemoto, D., D. A. Jones and A. R. Hardham (2003). "GFP-tagging of cell components reveals the dynamics of subcellular re-organization in response to infection of Arabidopsis by oomycete pathogens." Plant J **33**(4): 775-792.

Takemoto, D., D. A. Jones and A. R. Hardham (2006). "Re-organization of the cytoskeleton and endoplasmic reticulum in the Arabidopsis pen1-1 mutant inoculated with the non-adapted powdery mildew pathogen, Blumeria graminis f. sp. hordei." Mol Plant Pathol **7**(6): 553-563.

Voegele, R. T., C. Struck, M. Hahn and K. Mendgen (2001). "The role of haustoria in sugar supply during infection of broad bean by the rust fungus Uromyces fabae." Proc Natl Acad Sci U S A **98**(14): 8133-8138.

Waadt, R., L. K. Schmidt, M. Lohse, K. Hashimoto, R. Bock and J. Kudla (2008). "Multicolor bimolecular fluorescence complementation reveals simultaneous formation of alternative CBL/CIPK complexes in planta." Plant J **56**(3): 505-516.

Yu, J., J. Wang, W. Lin, S. Li, H. Li, J. Zhou, P. Ni, W. Dong, S. Hu, C. Zeng, J. Zhang, Y. Zhang, R. Li, Z. Xu, S. Li, X. Li, H. Zheng, L. Cong, L.

827 Lin, J. Yin, J. Geng, G. Li, J. Shi, J. Liu, H. Lv, J. Li, J. Wang, Y. Deng,
828 L. Ran, X. Shi, X. Wang, Q. Wu, C. Li, X. Ren, J. Wang, X. Wang, D.
829 Li, D. Liu, X. Zhang, Z. Ji, W. Zhao, Y. Sun, Z. Zhang, J. Bao, Y. Han,
830 L. Dong, J. Ji, P. Chen, S. Wu, J. Liu, Y. Xiao, D. Bu, J. Tan, L. Yang,
831 C. Ye, J. Zhang, J. Xu, Y. Zhou, Y. Yu, B. Zhang, S. Zhuang, H. Wei,
832 B. Liu, M. Lei, H. Yu, Y. Li, H. Xu, S. Wei, X. He, L. Fang, Z. Zhang,
833 Y. Zhang, X. Huang, Z. Su, W. Tong, J. Li, Z. Tong, S. Li, J. Ye, L.
834 Wang, L. Fang, T. Lei, C. Chen, H. Chen, Z. Xu, H. Li, H. Huang, F.
835 Zhang, H. Xu, N. Li, C. Zhao, S. Li, L. Dong, Y. Huang, L. Li, Y. Xi, Q.
836 Qi, W. Li, B. Zhang, W. Hu, Y. Zhang, X. Tian, Y. Jiao, X. Liang, J.
837 Jin, L. Gao, W. Zheng, B. Hao, S. Liu, W. Wang, L. Yuan, M. Cao, J.
838 McDermott, R. Samudrala, J. Wang, G. K. Wong and H. Yang (2005).
839 "The Genomes of Oryza sativa: a history of duplications." PLoS Biol
840 **3**(2): e38.

841

842

843

844

845

846

847

848

FIGURES

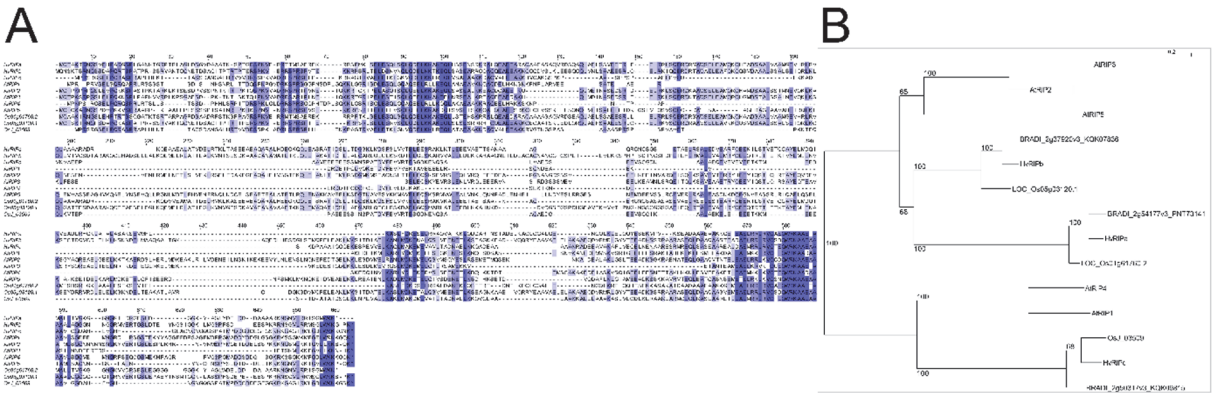

Figure 1. Alignment of amino acid sequences of barley RIP proteins with RIP proteins from Arabidopsis and rice. (A) Alignment was carried out with ClustalO and displayed with jalview (jalview 2.10.5). Color intensity relates to sequence identity. (B) A phylogenetic maximum likelihood tree was generated, including three additional RIP proteins from *Brachypodium distachyon* using the PhyML tool in the program seaview (v4.7).

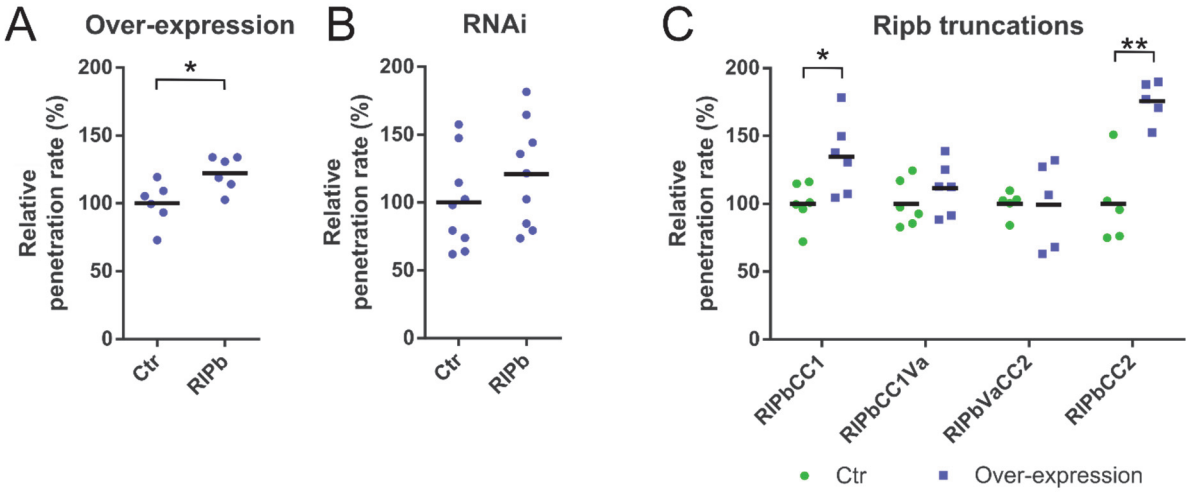

Figure 2. Effect of RIPb on the interaction of barley and *Bgh* was tested by biolistic transformation of epidermal cells of 7 days old barley leaves and determining the penetration rate of *Bgh* into the transformed cells 24 h after inoculation. Over-expression constructs for *RIPb* (A) as well as an RNAi silencing construct for *RIPb* (B) and over-expression constructs for *RIPb* truncations were introduced (C). As control, the respective empty vectors were used. Values represent the mean values of results of individual

868 experiments (n≥5) relative to the mean of the respective control set as 100
869 %. One asterisk indicates significance $P < 0.05$; two asterisk indicate
870 significance $P < 0.01$, Students t-test.
871
872

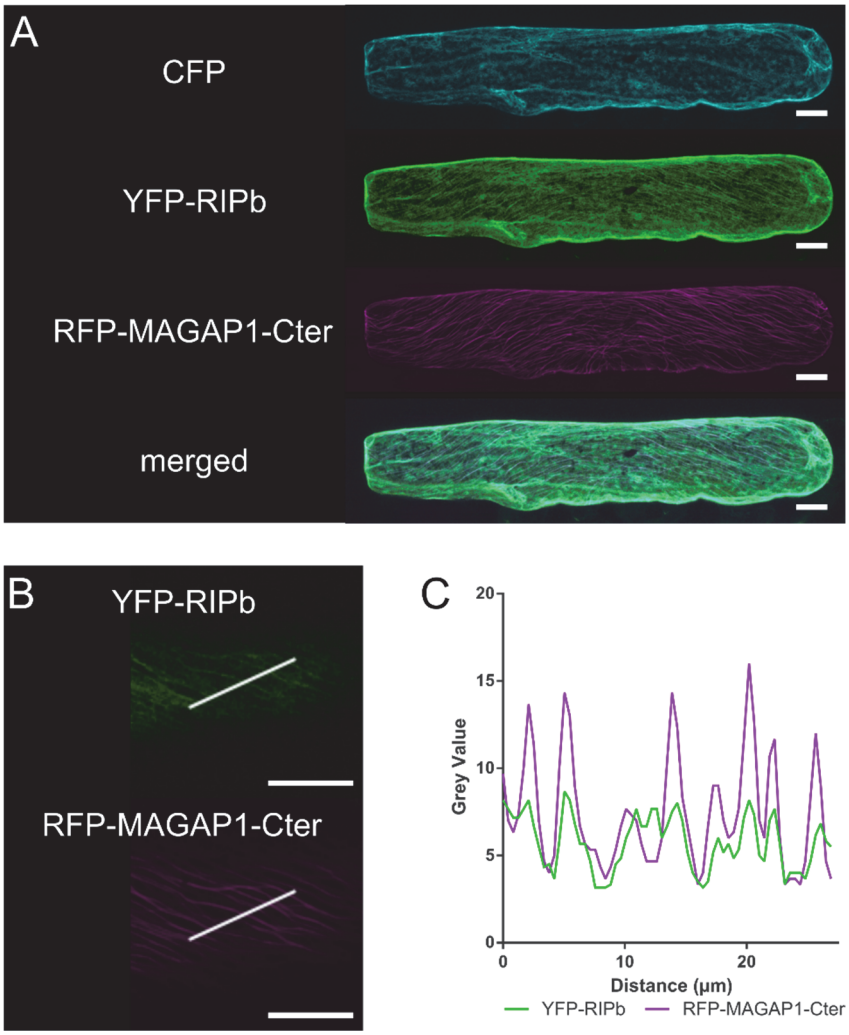

Figure 3. Subcellular localization of RIPb and *in planta*. (A) Barley epidermal cells were transiently co-transformed with CFP as a cytosolic marker, YFP-tagged RIPb (YFP-RIPb) and RFP-MAGAP1-Cter as a microtubule marker. Image shows z-stacks of XY optical sections of upper half of the cell. Bars represent 20µm. (B) An upper periclinal section of the image in (A) was used to measure signal intensities over a linear region of interest. Brightness of the images was equally increased for displaying purposes, but (C) Signal intensities of YFP-RIPb and RFP-MAGAP1-Cter over the region of interest highlighted in (B) were measured with the original data.

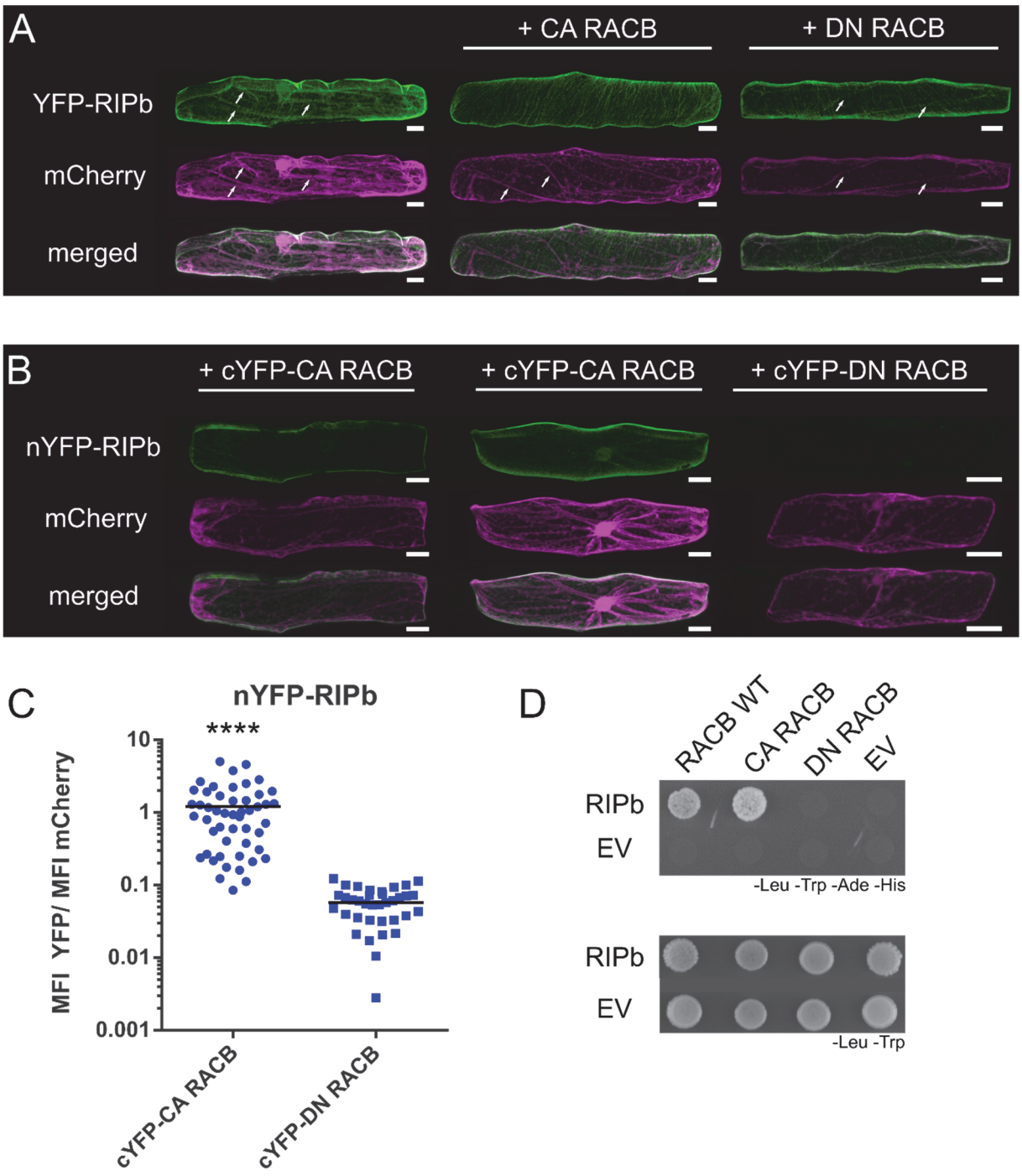

Figure 4. RACB and RIPb interact in yeast and in planta. (A) Single epidermal cells were transiently transformed by particle bombardment. YFP-RIPb and cytosolic transformation marker mCherry were expressed alone or co-expressed with constitutively activated RACB (CA RACB) or dominant negative RACB (DN RACB), respectively. Images were taken 24 hours after bombardment (hab) and show representative z-stacks of XY optical sections of the upper half of the cells. White arrows show cytosolic strands. White bars correspond to 20µm. (B) For BiFC experiments fusion-proteins of RIPb, CA RACB and DN RACB with split-YFP tags were coexpressed (B) images

were taken 24 hab. Images show z-stacks of XY optical sections of the upper half of the cells. White bars correspond to 20µm. (C) For quantification of BiFC experiments images were taken with constant settings and signal intensity (Mean Fluorescence Intensity, MFI) was measured over a region of interest at the cell periphery. The ratio between YFP and mCherry signal was calculated. The figure shows one out of two replicates with similar results. For each replicate >30 cells were measured. (D) RIPb was tested in a Yeast-Two-Hybrid assay for its interaction with barley wild type RACB (RACB WT), CA RACB and DN RACB. As control the interaction with the respective empty vectors (EV) was tested. For identification of interactions SD medium lacking leucine (-Leu), tryptophan (-Trp), adenine (-Ade) and histidine (-His) was used. For identification of transformed cells SD medium lacking leucine and tryptophan was used.

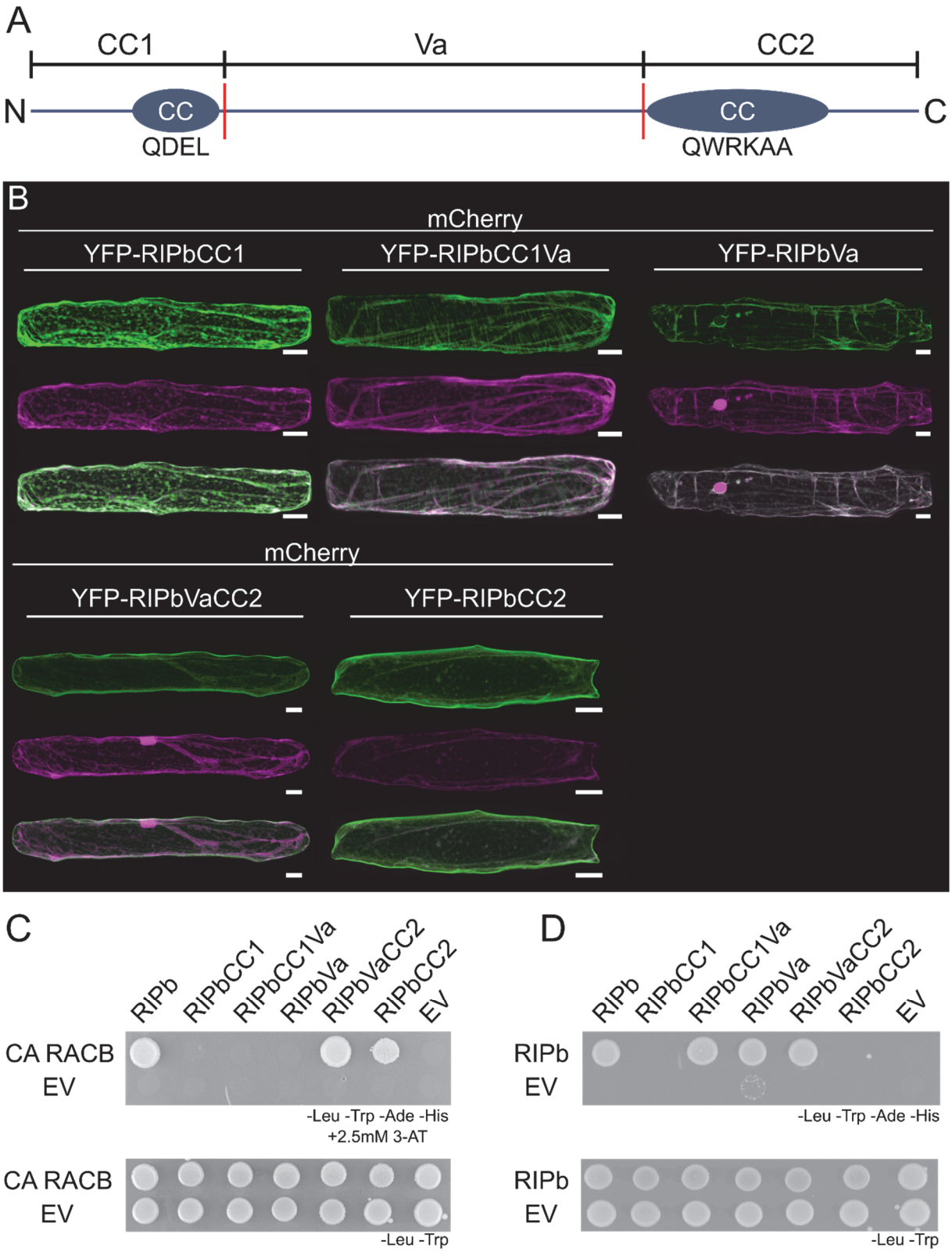

Figure 5. Structure function relationship of RIPb. (A) Domain structure and truncations of RIPb. The CC1-domain stretches from amino acid (aa) 1 to 132 and contains the N-terminal coiled-coil domain with the QDEL motif (CC, circles). The variable region (Va) starts at aa 133 at ends at aa 420. The CC2-domain stretches from aa 421 to the end at aa 612. The CC2-domain

916 also represents a coiled-coil structure and contains the QWRKAA motif. (B)
917 Single epidermal cells were transiently transformed with different RIPb
918 truncations tagged to YFP. Images show z-stacks of XY optical sections of
919 upper half of cells. White bars correspond to 20µm. (C) RIPb truncations
920 were tested in Yeast-Two-Hybrid assays for their interaction with
921 constitutively activated RACB (CA RACB) or RIPb (shown in D),
922 respectively. As controls, the interaction with the respective empty vector
923 (EV) was tested. For identification of interactions SD medium without
924 leucine (-Leu), tryptophan (-Trp), adenine (-Ade) and histidine (-His) was
925 used, together with 2,5mM 3-amino triazol to reduce background growth in
926 the combinations containing the RIPbVa truncation. For identification of
927 transformed cells SD medium without leucine and tryptophan was used.
928

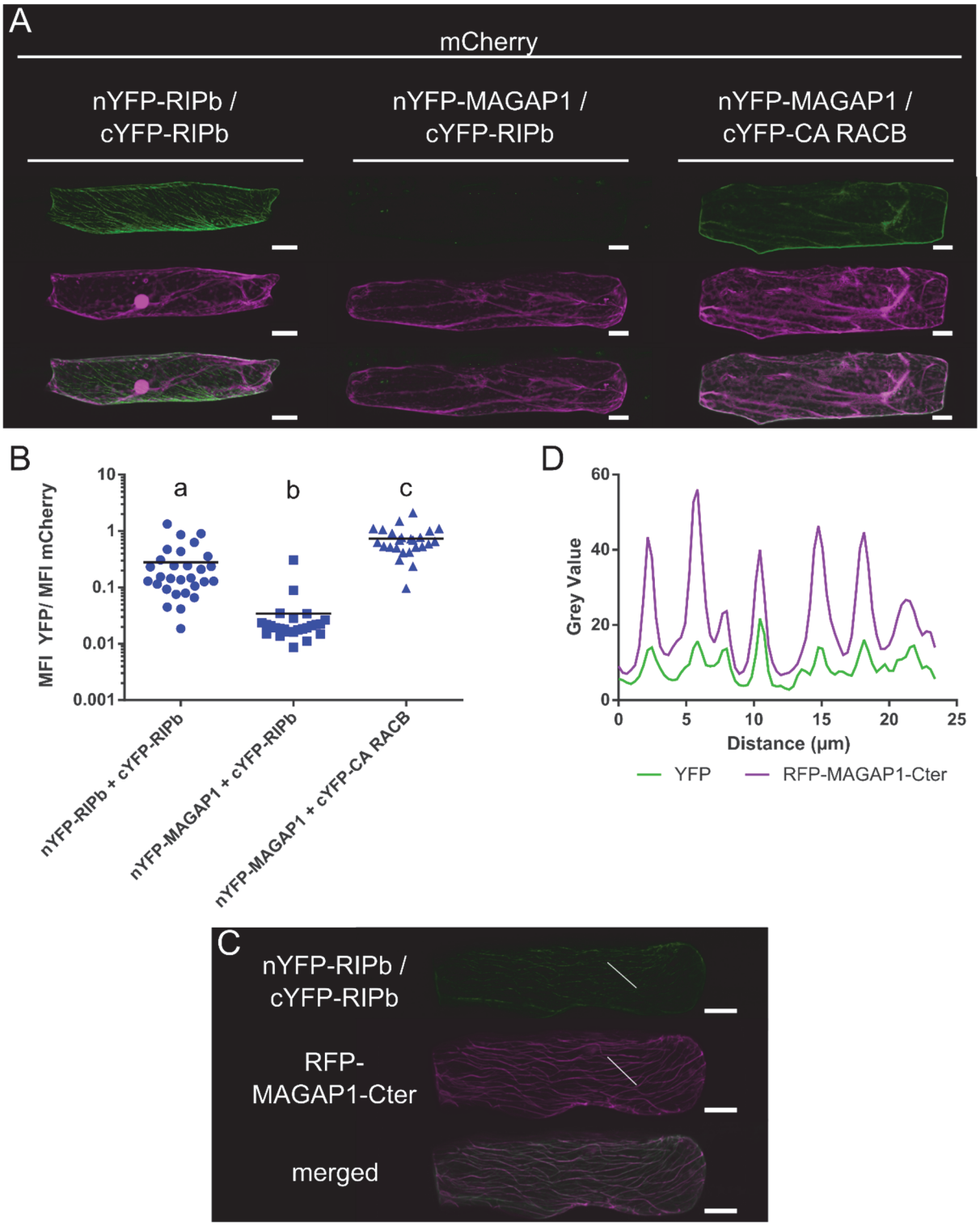

Figure 6. RIPb can interact with itself at microtubules. (A) Single epidermal cells were transiently transformed by particle bombardment with split-YFP constructs in the combination nYFP-RIPb and cYFP-RIPb, nYFP-MAGAP1 and cYFP-RIPb as well as nYFP-MAGAP1 and cYFP-RIPb. (C) For quantification of BiFC experiments images were taken with constant settings and signal intensity (Mean Fluorescence Intensity, MFI) was measured over a region of interest at the cell periphery. The ratio between YFP and

937 mCherry signal was calculated. (D) Co-expression of nYFP-RIPb and cYFP-
938 RIPb with RFP-MAGAP1-Cter. Image brightness was equally increased for
939 displaying purposes, but signal intensities (D) over a region of interest
940 (white line) were measured using original data. White bars correspond to
941 20µm.
942
943

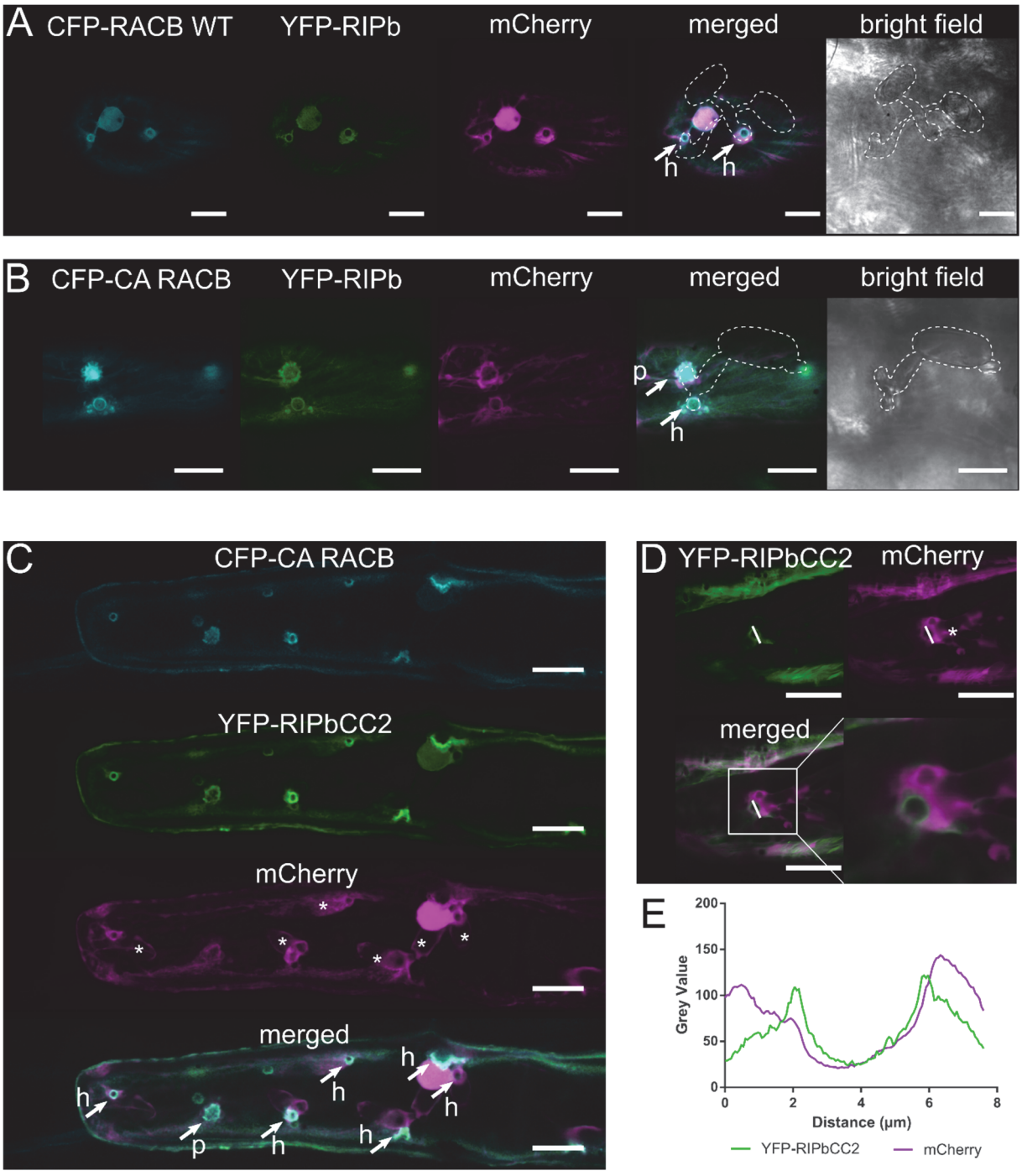

Figure 7. RIPb and RACB co-localize at sites of fungal attack. (A) Transiently transformed epidermis cells were inoculated with *Bgh*. YFP-RIPb co-localizes with CFP-RACB WT as well CFP-CA RACB (shown in B) at the site of fungal attack at 24 hours after inoculation. mCherry was used as a cytosolic marker. Fluorescence images on the left hand site show z-stacks of the upper part the cells. Transmission channel images show a single optical section. (C) YFP-RIPCC2 co-localizes with CFP-CA RACB 24 hours after inoculation at the site of fungal attack. mCherry was used as a cytosolic

954 marker. Arrows mark sites of fungal penetration attempts that either
955 succeeded with formation of a haustorium (h) or failed in a non-penetrated
956 papilla (p). Asterisks indicate haustorial bodies. (D) Single epidermal cells
957 were transiently transformed with YFP-RIPbCC2 and mCherry. Images were
958 taken 48 hours after inoculation with *Bgh.* Signal intensities at the haustorial
959 neck over the region of interest (white line) are shown in (E). Asterisks
960 indicate haustorial bodies. White bars correspond to 20µm.
961
962

963 **SUPPLEMENTAL MATERIAL**

964

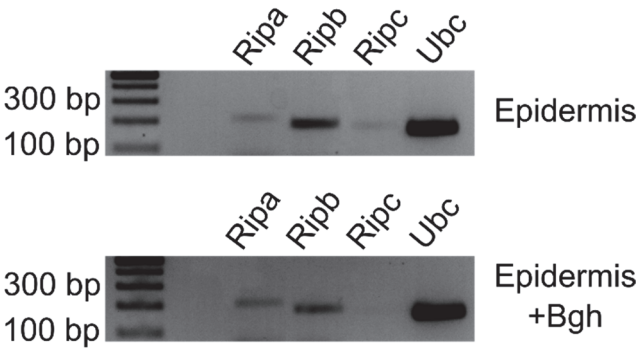

965

966 **Supplemental Fig. S1**. Semiquantitative PCR shows transcription levels of
967 *HvRIPa*, *HvRIPb* and *HvRIPc*. Samples were taken from epidermal layers of
968 barley leaves, either inoculated with *Bgh* or not. Equal amount of cDNA was
969 used to perform sqPCR. For each *RIP* primers were designed amplifying
970 around 200 bp from parts of the 5' sequnce of each *RIP*.

971

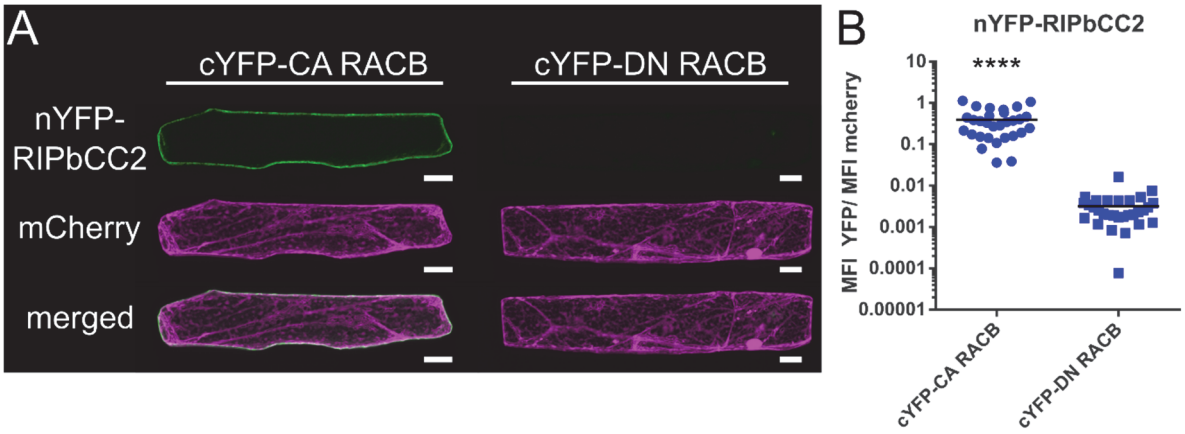

972

973 **Supplemental Fig. S2**. The CC2 domain of RIPb interacts with RACB *in*
974 *planta*. Single epidermal cells of barley leaves were transiently transformed
975 by particle bombardment with fusion proteins expressing split-YFP
976 constructs for BiFC. (A) nYFP-RIPbCC2 was either co-expressed with cYFP-
977 CA RACB or cYFP-DN RACB. mCherry served as transformation control.
978 White bars correspond to 20µm. (B) For quantification of YFP
979 complementation images were taken with constant settings and signal
980 intensity (Mean Fluorescence Intensity, MFI) was measured over a region
981 of interest at the cell periphery. The ratio between YFP and mCherry signal
982 was calculated (n=30).

983

984

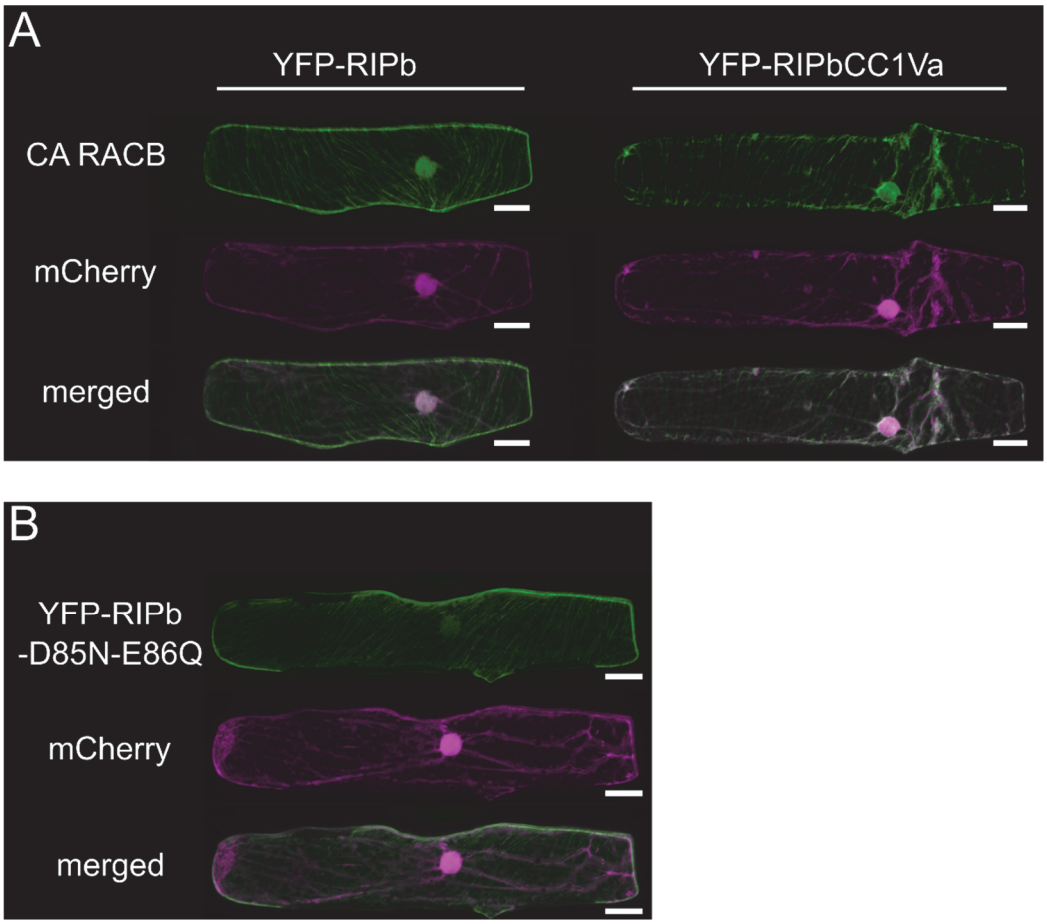

Supplemental Fig. S3. RIPbCC1Va cannot be recruited to the cell periphery by RACB. (A) Single epidermal cells were transiently transformed by particle bombardment with CA RACB, mCherry and either YFP-RIPb or YFP-RIPbC1Va. (B) Mutation D85N and E86Q were introduced into RIPb and a YFP-fusion protein was transiently expressed in single epidermal cells. White bars correspond to 20µm.

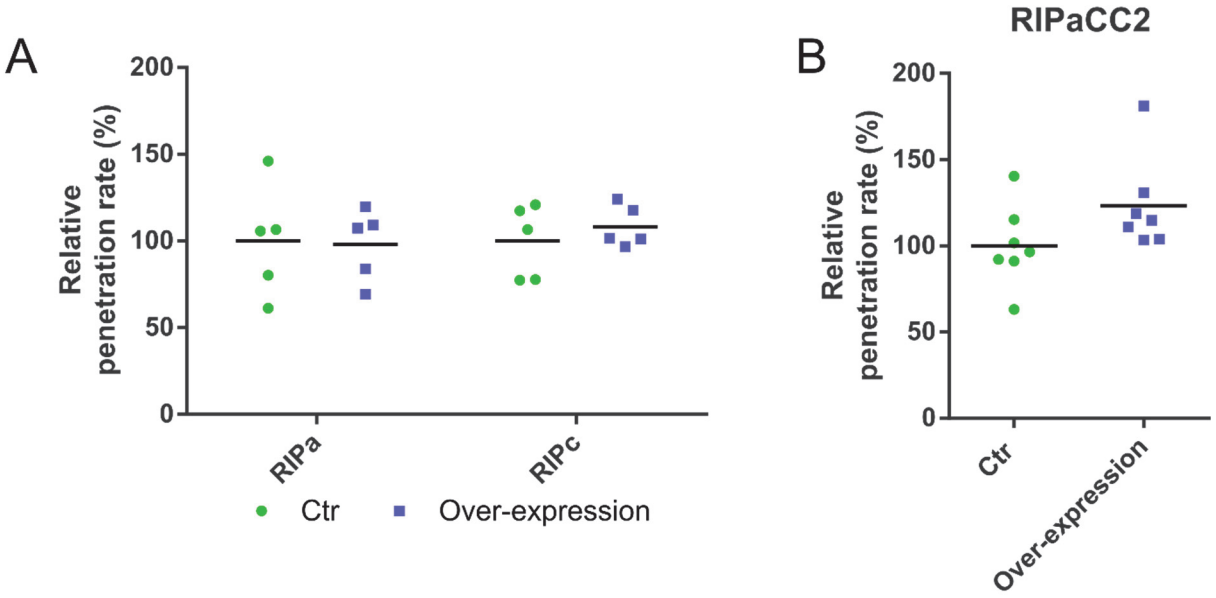

994

995 **Supplemental Fig. S4**. Effect of RIPa and RIPc on the interaction of barley
996 and *Bgh* was tested by biolistic transformation of epidermal cells of 7 days
997 old barley plants and determining the penetration rate of *Bgh* into the
998 transformed cells 24 h after inoculation. Over-expression constructs for
999 *RIPa* and *RIPc* (A) as well as an over-expression construct of *RIPaCC2* (B)
1000 were introduced (C). As control, the respective expression empty vectors
1001 were used. Values represent the mean values of results of individual
1002 experiments (n≥5) relative to the mean of the respective control set as 100
1003 %.

1004

1005

1006 *Supplemental Table 1* Primer list

Name	Sequence (5'-3')	Restriction sites /attachment sites	Product
Ripb-EcoRI_fwd	AGAATTCATGCAGAACTCAAAAACCAGTAG	EcoRI	*RIPb RIPbCC1*
Ripb-BamHI_rev	TGGATCCGGTCTCATGAGCTTCTTCAC	BamHI	*RIPb RIPbCC2*
Ripb-XbaI_fwd	TCTAGATATGCCGAGATCCAG	XbaI	*RIPb RIPbCC1*
Ripb-SalI_rev	AGTCGACCGGTCTCATGAGCT	SalI	*RIPb RIPbCC2*
Ripb-SpeI_fwd	TACTAGTTTCATGCAGAACTCAAAAACCAGTAG	SpeI	*RIPb*
RipbRNAi_fwd	ATCTAGACAGAGGCACGAAGGTGCCAAGCAC	XbaI	*RIPb-RNAi*
RipbRNAi_rev	TGTCGACCTTCAGGCATTCTTGCAACCGGGC	SalI	*RIPb-RNAi*
RipbC1-SalI_rev	TGTCGACTCAGAGATTGACAAGCTGGCA	SalI	*RIPbCC1*
RipbVa-XbaI_fwd	ATCTAGATATGTCAGCAGCAGAGGAGTCC	XbaI	*RIPbVa RIPbVaCC2*
RipbVa-SalI_rev	TGTCGACTCATTCGCTCAGCCCGTCTG	SalI	*RIPbVa RIPbCC1Va*
RipbC2-XbaI_fwd	ATCTAGACGAAATGCAGCCGGAGC	XbaI	*RIPbCC2*
GW-Ripb_fwd	GCAGGCTCAGGAATGCAGAACTCAAAAACCAGTAG		*RIPbCC1Va*
GW1-RipbC1Va-st_rev	GAAAGCTGGGTCCTCATTCGCTCAGCCCGTCTG		*RIPbCC1Va*
Gate2_F	GGGACAAGTTTGTACAAAAAAGCAGGCTCA	attB1	
Gate2_R	GGGGACCACTTTGTACAAGAAAGCTGGGTC	attB2	
RipaXbaI_fwd	TCTAGATATGCAGACAGCCAAGACAAG	XbaI	*RIPa*
RipaXbaI_rev	TCTAGATCATTTCTTCCACATTCCACTG	XbaI	*RIPa*
RipcXbaI_fwd	TCTAGATATGCAGAACTCAAAAACC	XbaI	*RIPc*
RipcPstI_rev	TCTGCAGTCACCTTCACTTGTTGCCC	PstI	*RIPc*
RipbC1BamHI_rev	TGGATCCTCAGAGATTGACAAGCTGGCAC	BamHI	*RIPbCC1*
RipbVaEcoRI_fwd	AGAATTCTCAGCAGCAGAGGAGTCC	EcoRI	*RIPbVa RIPbVaCC2*
RipbVaBamHI_rev	TGGATCCTCATTCGCTCAGCCCGTCTG	BamHI	*RIPbCC1Va RIPbVa*
RipbC2EcoRI_fwd	AGAATTCGAAATGCAGCCGGAGC	EcoRI	*RIPbCC2*
GW1-RipaCC2_fwd	GCAGGCTCAATGCAGGACGACGCGAGAACG		*RIPaCC2*
GW-Ripa_rev	GAAAGCTGGGTCTCATCATTTCTTCCACATTCCACTG		*RIPaCC2*
Ripa_sqPCR4_fwd	GCCAAGACAAGGAATGGCTC		*RIPa*
Ripa_sqPCR5_rev	GAGAGCTTCATGGGTGACCT		*RIPa*

Ripb_sqPCR9_fwd	CCCAGTTACTGAGAAGAAGCG		*RIPb*
Ripb_sqPCR10_rev	CAGCTTCAACGACACATCCTG		*RIPb*
Ripc_sqPCR4_fwd	GCTGCCAGAGAAGAGGCG		*RIPc*
Ripc_sqPCR5_rev	TTGGCGCCGACATGCTTC		*RIPc*
HvUBC2_fwd	TCTCGTCCCTGAGATTGCCCACAT		*UBC*
HvUBC2_rev	TTTCTCGGGACAGCAACACAATCTTCT		*UBC*

1007

1008